The N-terminal domain of N^{pro} of classical swine fever virus determines its stability and regulates type I interferon production

Junki Mine[1], Tomokazu Tamura[1], Kazuya Mitsuhashi[1], Masatoshi Okamatsu[1], Sujira Parchariyanon[2], Wasana Pinyochon[2], Nicolas Ruggli[3], Jon-Duri Tratschin[3], Hiroshi Kida[1,4,5], Yoshihiro Sakoda[1,5*]

[1]Laboratory of Microbiology, Department of Disease Control, Graduate School of Veterinary Medicine, Hokkaido University, Sapporo 060-0818, Japan

[2]National Institute of Animal Health, Kaset Klang, Chatuchak, Bangkok 10900, Thailand

[3]The Institute of Virology and Immunology IVI, Sensemattstrasse 293, CH-3147 Mittelhäusern, Switzerland

[4]Research Center for Zoonosis Control, Hokkaido University, Sapporo 001-0020, Japan

[5]Global Station for Zoonosis Control, Global Institution for Collaborative Research and Education (GI-CoRE), Hokkaido University, Sapporo 001-0020, Japan

[*]Corresponding author

Laboratory of Microbiology, Department of Disease Control, Graduate School of Veterinary Medicine, Hokkaido University, North 18, West 9, Kita-ku, Sapporo 060-0818, Japan

Phone: +81-11-706-5207; Fax: +81-11-706-5273

E-mail: sakoda@vetmed.hokudai.ac.jp

Summary word count: 242

The text word count: 5356, 7 figures, 1 tables, 3 supplementary figures

Running title: The N-terminal domain of CSFV N^{pro} determines its stability

Keywords: CSFV; N^{pro}; IFN-α/β; stability

Contents Category: Animal — Positive-strand RNA Viruses

The DDBJ accession number for the sequence of KPP/93 is LC016722.

SUMMARY

The viral protein N^{pro} is unique to the pestiviruses within the *Flaviviridae* family. After autocatalytic cleavage from the nascent polyprotein, N^{pro} suppresses type I interferon (IFN-α/β) induction by mediating proteasomal degradation of interferon regulatory factor 3 (IRF-3). Previous studies found that the N^{pro}-mediated IRF-3 degradation was dependent of a TRASH domain in the C-terminal half of N^{pro} coordinating zinc by means of the amino acid residues C112, C134, D136 and C138. Interestingly, four classical swine fever virus (CSFV) isolates obtained from diseased pigs in Thailand in 1993 and 1998 did not suppress IFN-α/β induction despite the presence of an intact TRASH domain. By systematic analyses, it was found that an amino acid mutation at position 40 or mutations at positions 17 and 61 in the N-terminal half of N^{pro} of these four isolates were related to the lack of IRF-3 degrading activity. Restoring a histidine at position 40 or both, a proline at position 17 and a lysine at position 61 based on the sequence of a functional N^{pro} contributed to higher stability of the reconstructed N^{pro} compared with the N^{pro} from the Thai isolate. This leaded to enhanced interaction of N^{pro} with IRF-3 along with its degradation by the proteasome. The results of the present study revealed that amino acid residues in the N-terminal domain of N^{pro} are involved in the stability of N^{pro}, in interaction of N^{pro} with IRF-3 and subsequent degradation of IRF-3, leading to down-regulation of IFN-α/β production.

INTRODUCTION

Viral infection triggers complex cellular antiviral defence mechanisms. Double-stranded RNA triggers the type I interferon (IFN-α/β) pathway, leading to antiviral responses such as the destruction of viral RNA, inhibition of cellular transcription and translation and promotion of apoptosis (Randall *et al*., 2008). IFN-α/β induction depends on a family of transcription factors, the interferon regulatory factors (IRFs) (Taniguchi *et al*., 2001). IRF-3 is ubiquitously expressed in the cytoplasm and activated in response to viral infection (Au *et al*., 1995). The activation of the pathway leads to phosphorylation, dimerization and translocation of IRF-3 into the nucleus, and to formation of the enhanceosome that binds to the IFN-α/β promoters (Honda *et al*., 2006; Saitoh *et al*., 2006). Previous studies have demonstrated that several viruses employ various strategies to counter this antiviral response. For instance, classical swine fever virus (CSFV) promotes IRF-3 degradation, hepatitis C virus inhibits IRF-3 phosphorylation, thogoto virus inhibits transcription complex assembly and influenza virus inhibits IRF-3 translocation into the nucleus (La Rocca *et al*., 2005; Hiliton *et al*., 2006; Haller *et al*., 2006; Jennings *et al*., 2005; Talon *et al*., 2000).

CSFV belongs to the genus *Pestivirus* of the family *Flaviviridae* together with bovine viral diarrhoea virus (BVDV) and border disease virus. CSFV possesses a single-stranded positive-sense RNA genome of approximately 12.3 kb with one large open reading frame flanked by a 5′ and 3′ untranslated region. It yields 12 cleavage products (N^{pro}, C, E^{rns}, E1, E2, p7, NS2, NS3, NS4A, NS4B, NS5A and NS5B) through co- and post-translational processing of the polyprotein by cellular and viral proteases (Lindenbach *et al*., 2007; Lamp *et al*., 2013). N^{pro} is a protein unique to pestiviruses and is generated autocatalytically by cleaving its own carboxyl terminus through its protease activity. The amino acid residues H49 and C69 in the N-terminal domain of N^{pro} form a catalytic diad responsible for the autoprotease activity (Gottipati *et al*., 2013; Zögg *et al*., 2013). N^{pro} is not essential for viral replication (Tratschin *et al*., 1998) but is involved in pathogenicity by suppressing IFN-α/β induction through IRF-3 degradation in host cells (Mayer *et al*., 2004; Hiliton *et al*., 2006; Bauhofer *et al*., 2007; Ruggli *et al*., 2009; Tamura *et al*., 2014). A TRASH zinc-binding domain located in the

C-terminal half of N^{pro} and involving the amino acid residues at positions 112, 134, 136 and 138, is required for mediating IRF-3 degradation (Ruggli *et al*., 2009; Szymanski *et al*., 2009; Tamura *et al*., 2014).

By means of N^{pro}, CSFV interferes with IFN-α/β induction, which can be measured with IFN-α/β indicators such as Newcastle disease virus (NDV). This is termed 'exaltation of NDV' (END) (Kumagai *et al*., 1958; Tamura *et al*., 2014). Four CSFV strains termed KPP/93, RBR/93, NKRS/98 and NKS/98 were isolated from diseased pigs in Thailand in 1993 and 1998. Surprisingly, these isolates were END-negative (END^-), representing the first END^- CSFV isolated in nature. All END^- strains described so far were derived in the laboratory (Shimizu *et al*., 1970; Sakoda *et al*., 1999). In the present study, we identified amino acid residues responsible for the suppression of IFN-α/β induction and elucidated the molecular mechanisms underlying this activity by N^{pro} of CSFVs isolated in Thailand.

RESULTS

Characterisation of CSFVs isolated in Thailand

To assess the involvement of N^{pro} of the Thai isolates in pathogenicity in pigs, three 4-week-old pigs were inoculated intramuscularly with $10^{7.0}$ $TCID_{50}$ of the KPP/93 strain and observed for 14 days. None of the inoculated pigs showed clinical symptoms. Although a small amount of virus was isolated from the tissue of one pig, no virus was isolated from other tissues and blood (Table 1). These data indicate that the pathogenicity of the KPP/93 strain in pigs is very low. Following this, we analysed the characteristics of the four Thai isolates in porcine cells. To clarify whether these isolates prevent IFN-α/β induction *in vitro*, porcine SK-L cells were infected at a multiplicity of infection (MOI) of 1.0 with the $vGPE^-$ and $vGPE^-$/N136D viruses as control, and with the four Thai isolates KPP/93, RBR/93, NKRS/98 or NKS/98. As expected, the $vGPE^-$ virus did not suppress IFN-α/β induction, as opposed to the $vGPE^-$/N136D virus, in which the zinc-binding domain important for IRF-3 degradation was restored with an aspartic acid at position 136, which mediated IRF-3 degradation in

accordance with the findings of previous reports (Ruggli *et al*., 2009, Tamura *et al*., 2014). All four Thai isolates induced IFN-α/β in SK-L cells, as observed with vGPE$^-$ (Fig. 1a). In addition, they did not induce IRF-3 degradation as observed with vGPE$^-$, while IRF-3 was not detected in SK-L cells inoculated with vGPE$^-$/N136D (Fig. 1b). These data show that the four Thai isolates KPP/93, RBR/93, NKRS/98 and NKS/98 do not suppress IFN-α/β induction.

Comparison of the amino acid sequences of N^{pro} of END$^+$ and END$^-$ CSFV strains

Previous studies demonstrated that the amino acid residues C112, C134, D136 and C138 of CSFV N^{pro} form a TRASH domain and are essential for the suppression of IFN-α/β induction (Ruggli *et al*., 2009; Szymanski *et al*., 2009). Four CSFV isolates in Thailand were classified into genotype 1.1 based on the E2 gene sequence (Fig. S1). These isolates shared 99% and 100% nucleotide sequence identity in E2 and N^{pro}, respectively (data not shown). The accession number of 11,677 nucleotides of the genome between the 5′ terminal domain and NS5B of the KPP/93 strain was deposited to the GenBank/EMBL/DDBJ public database (accession # LC016722). The amino acid sequences of N^{pro} of two out of the four strains isolated in Thailand, of three laboratory END$^-$ strains (ALD-END$^-$, Ames-END$^-$ and GPE$^-$), and of seven END-positive (END$^+$) strains (Alfort/187, Alfort/Tübingen, ALD, Brescia, C-strain, CAP and Eystrup) were compared. Amino acid residues specific to the CSFV isolated in Thailand were identified (Fig. 2, grey boxes). The alignment revealed H5Y, L8F, P17S, H40L, K61N, E113D and T151S as candidate mutations that may represent critical residues for the regulation of IFN-α/β induction. Interestingly, these seven amino acid positions were not located in the TRASH domain that was previously reported to be essential for N^{pro}-mediated IRF-3 degradation.

Identification of amino acid residues critical for the suppression of IFN-α/β induction

To identify amino acid residues of N^{pro} involved in the suppression of IFN-α/β induction, vA187-N^{pro}(KPP)-derived mutant viruses with substitutions in N^{pro} were constructed as described in

Fig. 3. The backbone virus vA187-N^{pro}(KPP) was a chimeric virus obtained by replacing the N^{pro} gene of vA187-1 (Ruggli *et al*., 1996) with the N^{pro} gene of the KPP/93 strain. The original vA187-1 virus down-regulates IFN-α/β production and is an established END^{+} virus *in vitro* (Ruggli *et al*., 2009). The nucleotide sequence identity of N^{pro} of the four CSFV isolates in Thailand was 100%, as described above; therefore, N^{pro} of the KPP/93 strain was considered as prototype for the four Thai isolates. IFN-α/β bioactivity was measured in the supernatant of cells inoculated with the different mutant viruses (Fig. 3). The vA187-N^{pro}(KPP)/D113E; S151T virus in which vA187-1 sequence was restored in the C-terminal part of KPP/93 N^{pro} did not suppress IFN-α/β production. Therefore, the five N-terminal amino acid residues at positions 5, 8, 17, 40 and 61 were suspected to be involved in this function. The histidine at position 40 of vA187-1 was close to the TRASH domain according to the 3D structure of N^{pro} (Fig. S2). The histidine at position 5 and the phenylalanine at position 8 were not plotted because of the lack of the N-terminal sixteen amino acids in 3D structure of N^{pro}. Interestingly, the L40H substitution in the KPP/93 N^{pro} backbone sequence was sufficient to confer the END^{+} phenotype as demonstrated with complete suppression of IFN-α/β production in SK-L cells infected with vA187-N^{pro}(KPP)/L40H. Interestingly also, vA187-N^{pro}(KPP)/Y5H; F8L; S17P; N61K did also suppress IFN-α/β production, suggesting that the remaining four amino acid residues were involved in this function too, independently of residue at position 40. By systematic analyses of mutant viruses carrying substitutions of either of these four residues alone or combination, we found that the two S17P and N61K substitutions together in the KPP/93 N^{pro} backbone sequence were sufficient to restore functional N^{pro} as measured by suppression of IFN-α/β production in SK-L cells inoculated with vA187-N^{pro}(KPP)/S17P; N61K (Fig. 3). In addition, IRF-3 protein was down-regulated in SK-L cells inoculated with vA187-N^{pro}(KPP)/L40H and vA187-N^{pro}(KPP)/S17P; N61K (Fig. 4). These data indicate that H40 or both, P17 and K61 are critical for the suppression of IFN-α/β induction by vA187-N^{pro}(KPP).

Time course of IRF-3 expression in cells infected with parent and mutant CSFVs

To elaborate on the contribution of the residues 17, 40 and 61 to the degradation of IRF-3 by N^{pro}, SK-L cells were infected with the END^- strain vA187-N^{pro}(KPP) which carries N^{pro} of the END^- KPP/93 in the vA187-1 backbone, and with the END^+ strains vA187-1, vA187-N^{pro}(KPP)/L40H carrying the mutation at amino acid position 40 or vA187-N^{pro}(KPP)/S17P; N61K carrying the mutations of amino acid residues 17 and 61. Cells were lysed at 0, 12, 24, 36, 48, 60, 72, 84, 96, 108 and 120 hours post-infection (hpi) and the extracts were analysed for IRF-3 expression. IRF-3 remained unchanged for the 5 days of the experiment in cells infected with vA187-N^{pro}(KPP) while it was clearly detectable for 24 hpi and then rapidly decreased to 3% of the initial IRF-3 levels by 36 hpi in cells infected with vA187-1 (Fig. 4). In cells infected with vA187-N^{pro}(KPP)/L40H, IRF-3 was detected at 0, 12, 24 and 36 hpi and then gradually decreased to less than 9% of the original IRF-3 level by 48 hpi. Similar decrease of IRF-3 expression was observed in cells infected with the KPP/93 strain carrying the double mutations at positions 17 and 61 [vA187-N^{pro}(KPP)/S17P; N61K] from 12 to 36 hpi, with 27% of the original IRF-3 level at 36 hpi. IRF-3 degradation in cells infected with these latter viruses was dependent on proteasomal activity as shown with the proteasome inhibitor MG-132 (Fig. S3). These data suggest that histidine at position 40 or both, proline at position 17 and lysine at position 61 are critical for N^{pro} to mediate proteasomal degradation of IRF-3 in infected cells.

Stability of N^{pro} of the KPP/93 strain and mutant viruses in cell culture

In a previous study, N^{pro} of the END^+ strain Alfort/187 carrying a single mutation at amino acid position 112 or 136, which are located in the TRASH domain was less stable than wild-type N^{pro} *in vitro* (Seago *et al*., 2010). To determine whether the amino acid residues at positions 17, 40 and 61 were responsible for the stability of N^{pro}, N^{pro} of the vA187-1 strain, KPP/93 strain and different amino acid mutants of N^{pro} of the KPP/93 virus were expressed in HEK293T cells and analysed for stability over time after treatment with the translation inhibitor cycloheximide (CHX) (Fig.5). vA187-1 N^{pro} carrying a single mutation at position 136 [N^{pro}(A187-1)/D136N] was mostly degraded after 12 hours in comparison with vA187-1 N^{pro}. This was in accordance with the findings of a previous report by

174 Seago *et al*. (2010). KPP/93 N^{pro} became undetectable within the first 4 h after CHX treatment. The
175 KPP/93 N^{pro} carrying the residues of the vA187-1 virus at the positions 17 and 61 [N^{pro}(KPP)/S17P;
176 N61K] was detected at 4 h after CHX treatment but became undetectable at 8 h. KPP/93 N^{pro}
177 carrying the histidine of vA187-1 at position 40 [N^{pro}(KPP)/L40H] or the three residues of vA187-1 at
178 positions 17, 40 and 61 [N^{pro}(KPP)/S17P; L40H; N61K] were detected for 12 h after CHX treatment,
179 similarly to vA187-1 N^{pro}. These data demonstrate that the amino acids of the END^{+} vA187-1 at
180 positions 40 or 17 and 61 enhance the stability of the KPP/93 N^{pro}.
181
182 **Interaction of IRF-3 with N^{pro} of the KPP/93 virus and mutants thereof**
183 A previous study demonstrated that IRF-3 was not degraded in porcine cells inoculated with the
184 vA187-D136N virus which carried a mutation at position 136 of N^{pro} in the TRASH domain, abolishing
185 zinc binding. In addition, the results of a mammalian two-hybrid assay showed that vA187-D136N
186 N^{pro} did not interact with IRF-3, while vA187-1 N^{pro} did (Ruggli *et al*., 2009). According to the results of
187 the present study, histidine at position 40 or both, proline at position 17 and lysine at position 61 are
188 required by N^{pro} for the suppression of IFN-α/β induction. Therefore, the importance of these amino
189 acid residues of N^{pro} for the interaction with IRF-3 was explored using the KPP/93 N^{pro} backbone and
190 a mammalian two-hybrid assay. Co-expression of the VP16 transactivator fused to IRF-3 and of the
191 GAL4 DNA-binding domain fused to vA187-1 N^{pro} resulted in luciferase expression from the reporter
192 plasmid due to the interaction of IRF-3 and N^{pro} (Fig. 6). As expected, vA187-1 N^{pro} carrying the
193 D136N mutation [N^{pro}(A187-1)/D136N] did not interact with IRF-3, in accordance with previous
194 findings (Ruggli *et al*., 2009). KPP/93 N^{pro} did not interact with IRF-3 either, similarly to vA187-D136N
195 N^{pro}. The mutant KPP/93 N^{pro} carrying a histidine at position 40 [N^{pro}(KPP)/L40H] resulted in
196 significantly higher luciferase activity than KPP/93 N^{pro}; however, the activity was not as high as with
197 vA187-1 N^{pro}. The mutant KPP/93 N^{pro} carrying the two residues of vA187-1 at positions 17 and 61
198 [N^{pro}(KPP)/S17P; N61K], showed low luciferase activity, which was comparable to that of the KPP/93
199 N^{pro}. Finally, the triple mutant KPP/93 N^{pro} carrying the residues of vA187-1 at positions 17, 40 and 61

200 [N^{pro}(KPP)/S17P; L40H; N61K] resulted in significantly higher luciferase activity than N^{pro}(KPP)/L40H,
201 comparable with the luciferase activity obtained with vA187-1 N^{pro}. Taken together, these data
202 indicate that, besides an intact TRASH domain, the amino acid residue at position 40 of N^{pro} is critical
203 for the interaction of N^{pro} with IRF-3, and that the amino acid residues at positions 17 and 61 act in
204 synergy with the residue at position 40 to mediate the interaction of N^{pro} with IRF-3.
205
206 **Discussion**
207 From 1993 to 1998, four END^- CSFVs (KPP/93, RBR/93, NKRS/98 and NKS/98 strains) were
208 isolated from diseased pigs in Thailand, while other CSFV strains isolated in nature were all END^+
209 strains until now. The KPP/93 strain showed low pathogenicity in pigs. In previous studies, the
210 suppression of IFN-α/β induction by N^{pro} was related to pathogenicity in pigs (Mayer *et al*., 2004;
211 Ruggli *et al*., 2009; Tamura *et al*., 2014), suggesting that inability of KPP/93 N^{pro} to suppress IFN-α/β
212 induction may contribute to the low pathogenicity of the KPP/93 strain in pigs. In the present study,
213 we identified amino acid residues of N^{pro} responsible for the suppression of IFN-α/β induction by N^{pro}.
214 We found that either the amino acid residue at position 40 or the combination of the amino acid
215 residues at positions 17 and 61 of N^{pro} were responsible for the suppression of IFN-α/β induction.
216 These three amino acid residues are located outside of the TRASH domain considering the crystal
217 structure of N^{pro} revealed by Gottipati *et al*. (2013), suggesting that besides the C-terminal half of N^{pro},
218 the N-terminal half of N^{pro} is also important for the suppression of IFN-α/β induction.
219 We then explored the molecular mechanisms underlying the suppression of IFN-α/β induction
220 mediated by these amino acid residues of N^{pro}. To this end, we analysed the kinetics of IRF-3
221 expression in porcine SK-L cells infected with chimeric viruses carrying N^{pro} of the KPP/93 strain and
222 mutants thereof in the vA187-1 backbone. No differences in the growth kinetics of CSFV vA187-1,
223 vA187-N^{pro}(KPP), vA187-N^{pro}(KPP)/L40H and vA187-N^{pro}(KPP)/S17P; N61K were observed during a
224 period of 120 hpi (data not shown). Nevertheless, IRF-3 was clearly down-regulated in cells infected
225 with vA187-1, vA187-N^{pro}(KPP)/L40H and vA187-N^{pro}(KPP)/S17P; N61K, compared with cells

infected with vA187-N^{pro}(KPP). To clarify the reasons for these differences, the stability of N^{pro} was examined. This was motivated by a recent study showing that N^{pro} of the END^{+} strain Alfort/187 carrying a single mutation at amino acid position 112 or 136 located in the TRASH domain, was less stable than wild-type N^{pro} (Seago *et al*., 2010). Thus, we assessed whether the amino acid residues at positions 17, 40 and 61 also influenced the stability of N^{pro}. N^{pro}(KPP)/L40H and N^{pro}(KPP)/S17P; N61K showed higher stability than the parental KPP/93 N^{pro} indicating that the amino acid residues at positions 17, 40 and 61 are involved in stabilising N^{pro}. vA187-1 N^{pro} with the D136N mutation [N^{pro}(A187-1)/D136N] showed reduced stability; however, the stability was higher than that of N^{pro}(KPP)/S17P; N61K conferring an END^{+} phenotype, while the vA187-1/D136N virus was END^{-}. These results suggest that while N^{pro}(KPP)/S17P; N61K can still mediate IRF-3 degradation despite slightly reduced stability, N^{pro}(A187-1)/D136N has lost the capacity to mediate IRF-3 degradation due to the mutation destroying the TRASH domain. In a previous study, N^{pro} of the END^{+} vA187-1 strain interacted with IRF-3 in cell culture as determined by a mammalian two-hybrid assay, and infection with this virus promoted IRF-3 degradation. On the other hand, N^{pro} of the END^{-} vA187-1/D136N virus did not interact with IRF-3, and this virus did not promote IRF-3 degradation (Ruggli *et al*., 2009). In the present study, a single amino acid mutation at position 40 of N^{pro}(KPP) was sufficient to restore interaction of N^{pro} with IRF-3, and two additional amino acid substitutions at positions 17 and 61 of N^{pro}(KPP)/L40H further enhanced the interaction of N^{pro}(KPP)/L40H with IRF-3. There was no interaction observed between N^{pro}(KPP)/S17P; N61K and IRF-3 using the mammalian two-hybrid assay despite the END^{+} phenotype conferred by this mutant N^{pro}, suggesting that further experiments are required to assess the interaction of N^{pro} with IRF-3 in more depth; in addition, the interaction of N^{pro} with other host factors needs also to be explored as suggested previously (Jefferson *et al*., 2014). Our data suggest that the differences in N^{pro}-mediated IRF-3 degradation in SK-L cells can be attributed to the degree of N^{pro} stability and to the strength of N^{pro} interaction with IRF-3.

Our results revealed that the stability of N^{pro} may influence the interaction of N^{pro} with IRF-3 and the subsequent down-regulation of IFN-α/β production. The amino acid residue at position 40 in the

N-terminal half of N^{pro} does clearly contribute to the stability of N^{pro}. A previous study of N^{pro} of BVDV demonstrated that this histidine at position 40 forms an ion-binding site for protein interactions together with the amino acid residues at positions 117 and 127 (Zögg *et al*., 2013). Therefore, the formation of this ion-binding site may act to stabilise N^{pro}. As described in Fig. 7, stable N^{pro}(KPP)/L40H results in a large amount of functional N^{pro} in cells, leading to efficient degradation of IRF-3 by the proteasome. In contrast, unstable N^{pro}(KPP) results in insufficient functional N^{pro} for IRF-3 degradation and for inhibition of IFN-α/β induction. Restoring the vA187-1 residues at positions 17 and 61 of N^{pro}(KPP) did only slightly enhance the stability of KPP/93 N^{pro}, resulting in a small amount of functional N^{pro} in cells. This small amount of N^{pro} was nevertheless sufficient to mediate degradation of IRF-3 and subsequent down-regulation of IFN-α/β production. N^{pro}(A187-1)/D136N showed higher stability than N^{pro}(KPP)/S17P; N61K although it was described to be defective in mediating IRF-3 degradation (Ruggli *et al*., 2009). This suggests that the lack of IRF-3 degradation by this TRASH domain mutant is indeed due to the lack of interaction with IRF-3 as described by Ruggli *et al*., (2009) rather than to N^{pro} instability although contribution of the latter cannot be excluded.

In conclusion, the present study reveals that the amino acid residues at positions 17, 40, and 61 in the N-terminal half of N^{pro} were contributed to the stability of N^{pro} and to the interaction of N^{pro} with IRF-3, leading to degradation of IRF-3 and subsequent down-regulation of IFN-α/β production. Thus, these data show that the N-terminal half and the C-terminal TRASH domain of N^{pro} are both involved with specific characteristics in the counteraction of type I IFN induction through mediating IRF-3 degradation.

METHODS

Cells

The porcine kidney cell line SK-L (Sakoda & Fukusho, 1998) was propagated in Eagle's minimum

essential medium (MEM) (Nissui, Tokyo, Japan) supplemented with 0.295% tryptose phosphate broth (TPB) (Becton Dickinson, San Jose, CA, USA), 10 mM *N,N*-bis-(2-hydroxyethyl)-2-aminoethanesulfonic acid (Sigma-Aldrich, St. Louis, MO, USA) and 10% horse serum (Invitrogen, Carlsbad, CA, USA). The SK6-MxLuc cell line carrying a Mx/Luc reporter gene (Ocaña-Macchi *et al.,* 2009) was propagated in MEM supplemented with 0.295% TPB and 7% horse serum. The human embryonic kidney cell line HEK293T was maintained in Dulbecco's MEM (Life Technologies, Carlsbad, CA, USA) and 10% foetal calf serum (Cambrex, Grand Island, NY, USA). All cells were incubated at 37°C in the presence of 5% CO_2.

Viruses

The CSFV KPP/93, RBR/93, NKRS/98 and NKS/98 strains were isolated from pigs in Kamphaeng Phet province in 1993, in Ratchaburi province in 1993, in Nakhon Ratchasima province in 1998 and in Nakhon Sawan province in 1998, respectively. The KPP/93 strain was isolated from diseased pigs showing clinical symptoms of CSF *i.e.* conjunctivitis, clustering, staggering, joint swelling and hemorrhagic skin lesion with a mortality of only 10%. After the isolation from the field, the KPP/93 strain was cloned by limiting dilution and passaged 5 times in porcine cells before this study. There is no other information about RBR/93, NKRS/98 and NKS/98 strains. The moderately virulent END^+ vA187-1 and the vA187-N^{pro}(KPP) virus which was obtained by replacing the N^{pro} gene in the vA187-1 backbone with the N^{pro} gene of the KPP/93 strain, were derived from the full-length cDNA pA187-1 (Ruggli *et al*., 1996) and pA187-N^{pro}(KPP), respectively. The vA187-N^{pro}(KPP)-derived mutant viruses were rescued from mutant cDNA plasmids that were constructed using the QuikChange XL Site-Directed Mutagenesis Kit (Agilent Technologies, Santa Clara, CA, USA) and oligonucleotide primers containing the respective mutation, applying standard techniques as described previously (Tamura *et al*., 2012). All cDNA-derived viruses were rescued as described previously (Moser *et al*., 1999; Tamura *et al*., 2012). In brief, plasmid constructs were linearised at the *SrfI* site located at the end of the viral genomic cDNA sequence, and RNA was obtained by

304 run-off transcription using the MEGAscript T7 kit (Ambion, Huntingdon, UK). After DNase I treatment
305 and purification on S-400 HR Sephadex columns (GE Healthcare, Buckinghamshire, UK), RNA was
306 quantified using a spectrophotometer (Amersham Bioscience Co., Ltd. UK) and used to
307 electroporate SK-L cells. The whole genomes of rescued viruses were verified by nucleotide
308 sequencing to exclude any accidental mutation. Rescued viruses were stored at −80°C.
309
310 **Sequencing**
311 Full-length cDNA clones and *in vitro*-rescued viruses were completely sequenced as described
312 previously (Tamura *et al*., 2012). In brief, nucleotide sequencing of cDNA clones and PCR fragments
313 of viral RNA was performed using the BigDye Terminator v3.1 Cycle Sequencing Kit (Life
314 Technologies) and a 3500 Genetic Analyzer (Life Technologies). Sequencing data were analysed
315 using GENETYX® Network version 12 (GENETYX, Tokyo, Japan).
316
317 **Virus titration**
318 Virus titres were determined by end-point dilution on SK-L cells and immunoperoxidase staining
319 using the anti-NS3 monoclonal antibody (mAb) 46/1, as described previously (Sakoda *et al*., 1998;
320 Kameyama *et al*., 2006). The titres were calculated using the formula of Reed and Muench (1938)
321 and expressed in 50% tissue culture infective dose ($TCID_{50}$)/ml.
322
323 **SDS-PAGE and western blotting**
324 SDS-PAGE and western blotting were performed as described previously (Tamura *et al*., 2014).
325 The concentration of SDS polyacrylamide gels was 15%. As primary antibodies, anti-porcine IRF-3
326 mAb 34/1 (Bauhofer *et al.*, 2007), anti-FLAG M2 mAb (Sigma-Aldrich) and anti-β actin antibody
327 (Cosmo Bio, Tokyo, Japan) were used. Immobilon Western Detection Reagents (Millipore, Bedford,
328 MA, USA) and the LumiVision PRO 400EX system (Aisin Seiki, Aichi, Japan) were used for the
329 signal detection.

330

331 **IFN bioassay**

332 The bioactivity of porcine IFN-α/β was assessed as described previously (Tamura *et al*., 2014). In
333 brief, supernatants of cells inoculated with viruses were inactivated using a UV crosslinker (ATTO,
334 Tokyo, Japan) and added to SK6-MxLuc cells. Recombinant porcine IFN-α/β produced in 293T cells
335 was used as a standard. The cell extracts were prepared with 100 μl of passive lysis buffer, and
336 firefly luciferase activities were measured using the Luciferase Assay System (Promega, Madison,
337 WI, USA) and a PowerScan4 microplate reader (DS Pharma Biomedical Co., Ltd., Osaka, Japan).
338 The activities were analysed using Gen5 software (DS Pharma Biomedical Co., Ltd.). Results were
339 recorded for three independent experiments and each experiment was performed in duplicate.
340 Statistically significant differences were detected using Student's *t* test.

341

342 **Experimental infection of pigs**

343 To assess the pathogenicity of the KPP/93 strain, three 4-week-old crossbred Landrace × Duroc ×
344 Yorkshire SPF pigs (Yamanaka Chikusan, Hokkaido, Japan) were intramuscularly injected with $10^{7.0}$
345 $TCID_{50}$ of the KPP/93 strain and observed for 14 days. From the three pigs kept for 14 days, blood
346 was collected in tubes containing EDTA (Terumo, Tokyo, Japan) on days 0, 3, 5, 7, 9, 11 and 14 pi for
347 virus titration. The pigs were euthanised with pentobarbital on day 14 pi, and tissues from tonsils,
348 kidneys and mesenteric lymph nodes were collected aseptically. The collected samples were
349 homogenised in MEM to obtain a 10% suspension for virus titration. Virus titres were expressed as
350 $TCID_{50}$/ml (blood) or gram (tissue). Neutralisation titres against the KPP/93 strain of sera collected
351 on days 14 pi were measured. This animal experiment was conducted in the BSL-3 facility of the
352 Graduate School of Veterinary Medicine, Hokkaido University, Sapporo, Japan accredited by
353 AAALAC International. The institutional animal care and use committee of the Graduate School of
354 Veterinary Medicine authorized animal experiment of pigs (approval number: 12-0013). All
355 experiments were performed according to the guidelines of this committee.

Time course analysis

The SK-L cells seeded in 6-well plates were inoculated with viruses at an MOI of 5.0 and incubated at 37°C in the presence of 5% CO_2. At 0, 12, 24, 36, 48, 60, 72, 84, 96, 108 and 120 hpi, the supernatants were collected for virus titration and IFN-α/β quantification. The cell lysates were prepared for the detection of the IRF-3 protein. The intensity of the specific band of IRF-3 was quantified using the image analysis software Image J (Schneider *et al*., 2012)

Stability test of N^{pro} in HEK293T cells

For the measurement of the stability of N^{pro}, HEK293T cells were seeded in 24-well plates at a density of 10^5 cells per well. After 24 h, the cells were transfected with 1 μg of pCI-M-FLAG-N^{pro}-derived plasmids. FLAG-N^{pro} was expressed at 37°C for 24 h. After incubation, the expression was stopped by adding 200 ng of the protein synthesis inhibitor CHX (Sigma-Aldrich). Cell lysates were prepared with the passive lysis buffer at 0, 4, 8 and 12 h after CHX treatment. FLAG-N^{pro} was detected by western blotting.

Mammalian two-hybrid assay.

The mammalian two-hybrid assays were performed as described previously (Ruggli *et al*., 2009). In brief, 293T cells were transfected with pFN10A(ACT)-IRF3 expressing porcine IRF-3 fused to the VP16 transactivator and with pFN11A(BIND)-derived plasmids expressing a fusion of the GAL4 DNA-binding domain and N^{pro} protein of CSFVs. The empty vectors pACT and pBIND and the corresponding plasmids expressing MyoD and Id (Promega) served as controls. Cells were incubated for 24 h at 37°C in the presence of 5% CO_2 prior to extraction, and luciferase activity was measured as mentioned above. Results were recorded for three independent experiments, and each experiment was performed in duplicate. Statistically significant differences were calculated with the Student's *t* test.

Acknowledgements

We thank Dr. Kay Choi (The University of Texas Medical Branch, Galveston, USA) for the protein data of N^{pro}. We also thank N. Nagashima and Y. Fujimoto for excellent technical support and continuous assistance. The present work was partly supported by the Program for Leading Graduate Schools (F01) from Japan Society for the Promotion of Science (JSPS) and by the Swiss National Science Foundation grant # 3100A0-116608.

REFERENCES

Au, W. C., Moore, P. A., Lowther, W., Juang, Y. T. & Pitha, P. M. (1995). Identification of a member of the interferon regulatory factor family that binds to the interferon-stimulated response element and activates expression of interferon-induced genes. *Proc Natl Acad Sci U S A* **92**, 11657-11661.

Bauhofer, O., Summerfield, A., Sakoda, Y., Tratschin, J. D., Hofmann, M. A. & Ruggli, N. (2007). Classical swine fever virus N^{pro} interacts with interferon regulatory factor 3 and induces its proteasomal degradation. *J Virol* **81**, 3087-3096.

Gottipati, K., Ruggli, N., Gerber, M., Tratschin, J. D., Benning, M., Bellamy, H. & Choi, K. H. (2013). The structure of classical swine fever virus N^{pro}: a novel cysteine Autoprotease and zinc-binding protein involved in subversion of type I interferon induction. *PLoS Pathog* **9**, e1003704.

Haller, O., Kochs, G. & Weber, F. (2006). The interferon response circuit: induction and suppression by pathogenic viruses. *Virology* **344**, 119-130.

Hilton, L., Moganeradj, K., Zhang, G., Chen, Y. H., Randall, R. E., McCauley, J. W. & Goodbourn, S. (2006). The N^{pro} product of bovine viral diarrhoea virus inhibits DNA binding by interferon regulatory factor 3 and targets it for proteasomal degradation. *J Virol* **80**, 11723-11732.

Honda, K., Takaoka, A. & Taniguchi, T. (2006). Type I interferon gene induction by the interferon regulatory factor family of transcription factors. *Immunity* **25**, 349-360.

Jefferson, M., Donaszi-Ivanov, A., Pollen, S., Dalmay, T., Saalbach, G. & Powell, P. P. (2014). Host factors that interact with the pestivirus N-terminal protease, N^{pro}, are components of the ribonucleoprotein complex. *J Virol* **88**, 10340-10353.

Jennings, S., Martínez-Sobrido, L., García-Sastre, A., Weber, F. & Kochs, G. (2005). Thogoto virus ML protein suppresses IRF3 function. *Virology* **331**, 63-72.

Kameyama, K., Sakoda, Y., Tamai, K., Igarashi, H., Tajima, M., Mochizuki, T., Namba, Y. & Kida, H. (2006). Development of an immunochromatographic test kit for rapid detection of bovine viral diarrhoea virus antigen. *J Virol Methods* **138**, 140-146.

Kumagai, T., Shimizu, T. & Matumoto, M. (1958). Detection of hog cholera virus by its effect on Newcastle disease virus in swine tissue culture. *Science* **128**, 366.

La Rocca, S. A., Herbert, R. J., Crooke, H., Drew, T. W., Wileman, T. E. & Powell, P. P. (2005). Loss of interferon regulatory factor 3 in cells infected with classical swine fever virus involves the N-terminal protease, N^{pro}. *J Virol* **79**, 7239-7247.

Lamp, B., Riedel, C., Wentz, E., Tortorici, M. A. & Rümenapf, T. (2013). Autocatalytic cleavage within classical swine fever virus NS3 leads to a functional separation of protease and helicase. *J Virol* **87**, 11872-11883.

Lindenbach, B.D., Thiel, H.J., Rice, C.M., (2007). Flaviviridae: the viruses and their replicon, p. 1101-1152. In D.M. Knipe and P.M. Howley (ed), *Fields Virology, 5th ed*., vol. 1. Lippincott-Raven Publishers, Philadelphia, PA.

Mayer, D., Hofmann, M. A. & Tratschin, J. D. (2004). Attenuation of classical swine fever virus by deletion of the viral N^{pro} gene. *Vaccine* **22**, 317-328.

Moser, C., Stettler, P., Tratschin, J. D. & Hofmann, M. A. (1999). Cytopathogenic and noncytopathogenic RNA replicons of classical swine fever virus. *J Virol* **73**, 7787-7794.

Ocaña-Macchi, M., Bel, M., Guzylack-Piriou, L., Ruggli, N., Liniger, M., McCullough, K. C., Sakoda, Y., Isoda, N., Matrosovich, M. & Summerfield, A. (2009). Hemagglutinin-dependent tropism of H5N1 avian influenza virus for human endothelial cells. *J Virol* **83**, 12947-12955.

Randall, R. E. & Goodbourn, S. (2008). Interferons and viruses: an interplay between induction, signalling, antiviral responses and virus countermeasures. *J Gen Virol* **89**, 1-47.

Ruggli, N., Tratschin, J. D., Mittelholzer, C. & Hofmann, M. A. (1996). Nucleotide sequence of classical swine fever virus strain Alfort/187 and transcription of infectious RNA from stably cloned full-length cDNA. *J Virol* **70**, 3478-3487.

Ruggli, N., Summerfield, A., Fiebach, A. R., Guzylack-Piriou, L., Bauhofer, O., Lamm, C. G., Waltersperger, S., Matsuno, K., Liu, L., Gerber, M., Choi, K. H., Hofmann, M. A., Sakoda, Y. & Tratschin, J. D. (2009). Classical swine fever virus can remain virulent after specific elimination of the interferon regulatory factor 3-degrading function of N^{pro}. *J Virol* **83**, 817-829.

Reed, L. & Muench, H. (1938). A simple method of estimating fifty per cent endpoints. *Am. J. Epidemiol* **27**, 493-497

Saitoh, T., Tun-Kyi, A., Ryo, A., Yamamoto, M., Finn, G., Fujita, T., Akira, S., Yamamoto, N., Lu, K. P. & Yamaoka, S. (2006). Negative regulation of interferon-regulatory factor 3-dependent innate antiviral response by the prolyl isomerase Pin1. *Nat Immunol* **7**, 598-605.

Sakoda, Y. & Fukusho, A. (1998). Establishment and characterization of a porcine kidney cell line, FS-L3, which forms unique multicellular domes in serum-free culture. *In Vitro Cell Dev Biol Anim* **34**, 53-57.

Sakoda, Y., Ozawa, S., Damrongwatanapokin, S., Sato, M., Ishikawa, K. & Fukusho, A. (1999). Genetic heterogeneity of porcine and ruminant pestiviruses mainly isolated in Japan. *Vet Microbiol* **65**, 75-86.

Schneider, C. A., Rasband, W. S. & Eliceiri, K. W. (2012). NIH Image to ImageJ: 25 years of image analysis. *Nat Methods* **9**, 671-675.

Seago, J., Goodbourn, S. & Charleston, B. (2010). The classical swine fever virus N^{pro} product is degraded by cellular proteasomes in a manner that does not require interaction with interferon regulatory factor 3. *J Gen Virol* **91**, 721-72.

Shimizu, Y., Furuuchi, S., Kumagai, T. & Sasahara, J. (1970). A mutant of hog cholera virus inducing interference in swine testicle cell cultures. *Am J Vet Res* **31**, 1787-1794.

Szymanski, M. R., Fiebach, A. R., Tratschin, J. D., Gut, M., Ramanujam, V. M., Gottipati, K., Patel, P., Ye, M., Ruggli, N. & Choi, K. H. (2009). Zinc binding in pestivirus N^{pro} is required for interferon regulatory factor 3 interaction and degradation. *J Mol Biol* **391**, 438-449.

Talon, J., Horvath, C. M., Polley, R., Basler, C. F., Muster, T., Palese, P. & García-Sastre, A. (2000). Activation of interferon regulatory factor 3 is inhibited by the influenza A virus NS1 protein. *J Virol* **74**, 7989-7996.

Tamura, T., Sakoda, Y., Yoshino, F., Nomura, T., Yamamoto, N., Sato, Y., Okamatsu, M., Ruggli, N. & Kida, H. (2012). Selection of classical swine fever virus with enhanced pathogenicity reveals synergistic virulence determinants in E2 and NS4B. *J Virol* **86**, 8602-8613.

Tamura, T., Nagashima, N., Ruggli, N., Summerfield, A., Kida, H. & Sakoda, Y. (2014). N^{pro} of classical swine fever virus contributes to pathogenicity in pigs by preventing type I interferon induction at local replication sites. *Vet Res* **45**, 47.

Taniguchi, T., Ogasawara, K., Takaoka, A. & Tanaka, N. (2001). IRF family of transcription factors as regulators of host defense. *Annu Rev Immunol* **19**, 623-655.

Tratschin, J. D., Moser, C., Ruggli, N. & Hofmann, M. A. (1998). Classical swine fever virus leader proteinase N^{pro} is not required for viral replication in cell culture. *J Virol* **72**, 7681-7684.

Zögg, T., Sponring, M., Schindler, S., Koll, M., Schneider, R., Brandstetter, H. & Auer, B. (2013). Crystal structures of the viral protease N^{pro} imply distinct roles for the catalytic water in catalysis. *Structure* **21**, 929-938.

480 **Table**

Table 1. Virus recovery and neutralization titres from pigs inoculated with the KPP/93 strain.

Virus	Pig No.	Blood (log $TCID_{50}$/ml) on day pi						Tissue (log $TCID_{50}$/g) on days 14 pi			Neutralization titre on days 14 pi
		3	5	7	9	11	14	Tonsil	Kidney	Mesenteric lymph node	
KPP/93	1	−*	−	−	−	−	−	<1.8	−	−	1
	2	−	−	−	−	−	−	−	−	−	2
	3	−	−	−	−	−	−	−	−	−	1

481 * −: not isolated.

Figure legends

Fig. 1. IFN-α/β production and IRF-3 expression in swine cells infected with different END$^-$ and END$^+$ CSFV strains

Porcine SK-L cells were inoculated at an MOI of 1.0 with the CSFV strains KPP/93, RBR/93, NKRS/98, NKS/98, the END$^-$ CSFV strain vGPE$^-$ and the END$^+$ strain vGPE$^-$/N136D. After 5 days of incubation at 37°C in the presence of 5% CO_2, the supernatants were collected for quantification of IFN-α/β bioactivity (a), and the cells were lysed for analysis of IRF-3 expression (b). (a) The IFN-α/β bioactivity was measured in duplicate using the SK6-MxLuc reporter cells. The data represent the mean from three independent experiments, and the error bars show the standard errors. The significance of the differences was calculated using Student's *t* test. '*' indicates $p < 0.05$. (b) The cell extracts were prepared with passive lysis buffer and analysed by SDS-PAGE and Western blotting as described in materials and methods. IRF-3 was detected with the monoclonal antibody 34/1 against porcine IRF-3 shown with an arrow.

Fig. 2. Amino acid sequence alignment of N^{pro} of selected END$^+$ and END$^-$ CSFV strains

The N^{pro} amino acid sequences of selected END$^+$ CSFV strains which suppress IFN-α/β induction (Alfort/187, Alfort/Tübingen, ALD, Brescia, C-strain, CAP, and Eystrup), and of selected END$^-$ strains that suppress IFN-α/β induction (KPP/93, NKS/98, ALD-END$^-$, Ames-END$^-$ and GPE$^-$) are aligned. The GenBank accession numbers are as follows: Alfort/187, X87939; Alfort/Tübingen, J04358; Eystrup, AF326963; Brescia, AF091661; C-strain, Z46258; CAP, X96550; ALD, D49532; GPE$^-$, D49533. The N^{pro} sequences of the ALD-END$^-$ and Ames-END$^-$ strains were published previously (Ruggli *et al*., 2009). The amino acid numbering corresponds to the Alfort/187 sequence. The grey boxes highlight the amino acids unique to KPP/93 and NKS/98. The dotted boxes indicate the amino acids at position 112, 134, 136 and 138, located in the TRASH domain.

Fig. 3. Production of IFN-α/β in supernatants of SK-L cells inoculated with vA187-1,

vA187-N^{pro}(KPP) or mutant viruses

The swine SK-L cells were inoculated at an MOI of 1.0 with vA187-1, vA187-N^{pro}(KPP) or 12 mutant viruses. The vA187-N^{pro}(KPP) virus was generated by replacing the N^{pro} gene in the END^+ vA187-1 backbone with the N^{pro} gene of the END^- KPP/93 strain. Twelve mutant viruses were constructed by selected amino acid mutagenesis in N^{pro} of the vA187-N^{pro}(KPP) virus. SK-L cells infected with the different viruses were incubated at 37°C in the presence of 5% CO_2 for 5 days. IFN-α/β bioactivity in the cell supernatants was measured in duplicate using the SK6-MxLuc reporter gene assay. The data represent the mean from three independent experiments, and the error bars show the standard errors. The significance of the differences was calculated using Student's *t* test. '*' indicates $p < 0.05$.

Fig. 4. Time course of IRF-3 expression in cells infected with parent and mutant CSFV

SK-L cells were mock infected or inoculated with the vA187-N^{pro}(KPP), vA187-N^{pro}(KPP)/L40H, vA187-N^{pro}(KPP)/S17P; N61K and vA187-1 viruses. The cells were lysed at 0, 12, 24, 36, 48, 60, 72, 84, 96, 108 and 120 hpi. IRF-3 and β-actin were detected with the monoclonal antibody against porcine IRF-3 (34/1) and against β-actin, respectively.

Fig. 5. Stability of N^{pro} and mutant N^{pro} in HEK293T cells

HEK293T cells were transfected with pCI-M-FLAG-N^{pro}-derived plasmids expressing the original or mutant N^{pro} [N^{pro}(A187-1), N^{pro}(KPP), N^{pro}(KPP)/L40H, N^{pro}(KPP)/S17P; N61K, N^{pro}(KPP)/S17P; L40H, N61K and N^{pro}(A187-1)/D136N] tagged with a N-terminal FLAG epitope. Twenty-four hours after transfection, CHX was added to stop translation. The cells were extracted at 0, 4, 8 and 12 h after CHX treatment for the detection of FLAG-N^{pro} by Western blot with the anti-FLAG M2 monoclonal antibody.

Fig. 6. Evaluation of the interaction of the N^{pro} protein with IRF-3 by mammalian two-hybrid assay

534 HEK293T cells were co-transfected with pFN10A(ACT)-derived plasmids expressing IRF-3 fused to
535 the VP16 transactivator and with pFN11A(BIND)-derived plasmids expressing different forms of N^{pro}
536 [N^{pro}(A187-1), N^{pro}(KPP), N^{pro}(KPP)/L40H, N^{pro}(KPP)/S17P; N61K, N^{pro}(KPP)/S17P; L40H, N61K and
537 N^{pro}(A187-1)/D136/N] fused to the GAL4 DNA-binding domain. The empty vectors pACT and pBIND
538 served as controls. After 24 h of incubation, the cells were lysed and the firefly luciferase activity was
539 measured. The results are shown as relative luciferase activity compared with N^{pro}(A187-1). The data
540 represent the mean from three independent experiments, and the error bars show the standard
541 errors. The significance of the differences was calculated using Student's *t* test. '*' indicates $p < 0.05$.
542
543 **Fig. 7. Model of the molecular mechanisms of suppression of IFN-α/β induction by N^{pro}**
544 In cells infected with vA187-N^{pro}(KPP), N^{pro} is rapidly degraded and double-stranded RNA triggers
545 the activation of the IRF-3 phosphorylation pathway according to mechanisms described by Honda
546 *et al*. (2006), leading to IFN-β production. In cells infected with vA187-1 or vA187-N^{pro}(KPP)/L40H,
547 N^{pro} is stable, which results in a large amount of functional N^{pro} leading to efficient IRF-3 degradation
548 by the proteasome to suppress IFN-β production. In cells infected with vA187-N^{pro}(KPP)/S17P; N61K,
549 despite limited stability of N^{pro}, there is sufficient functional N^{pro} to degrade IRF-3 resulting in
550 suppression of IFN-β production.

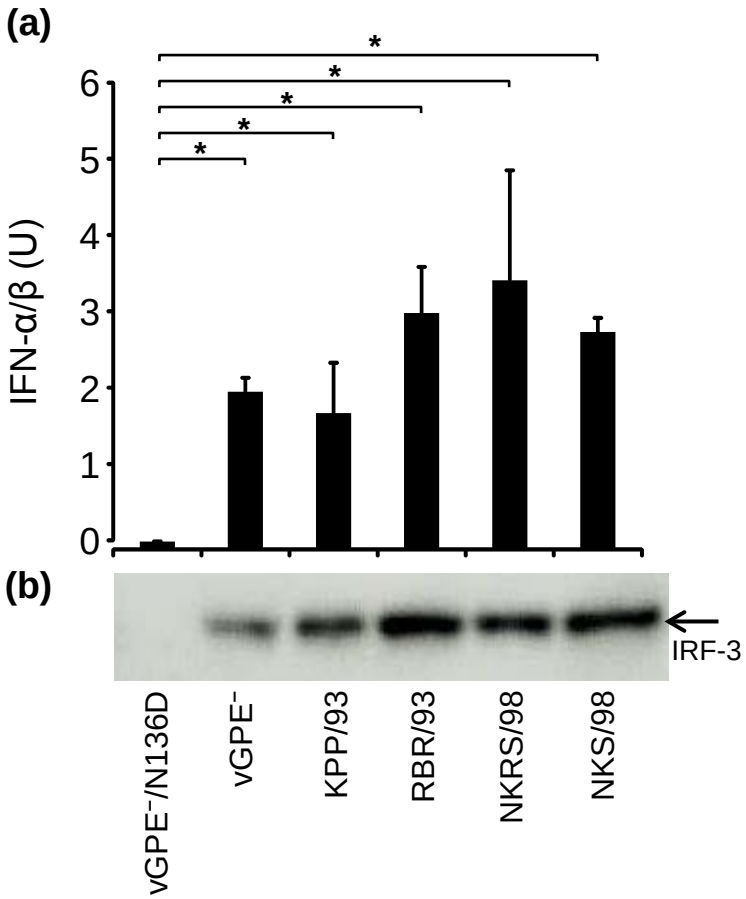

Figure 1, Mine *et al*.

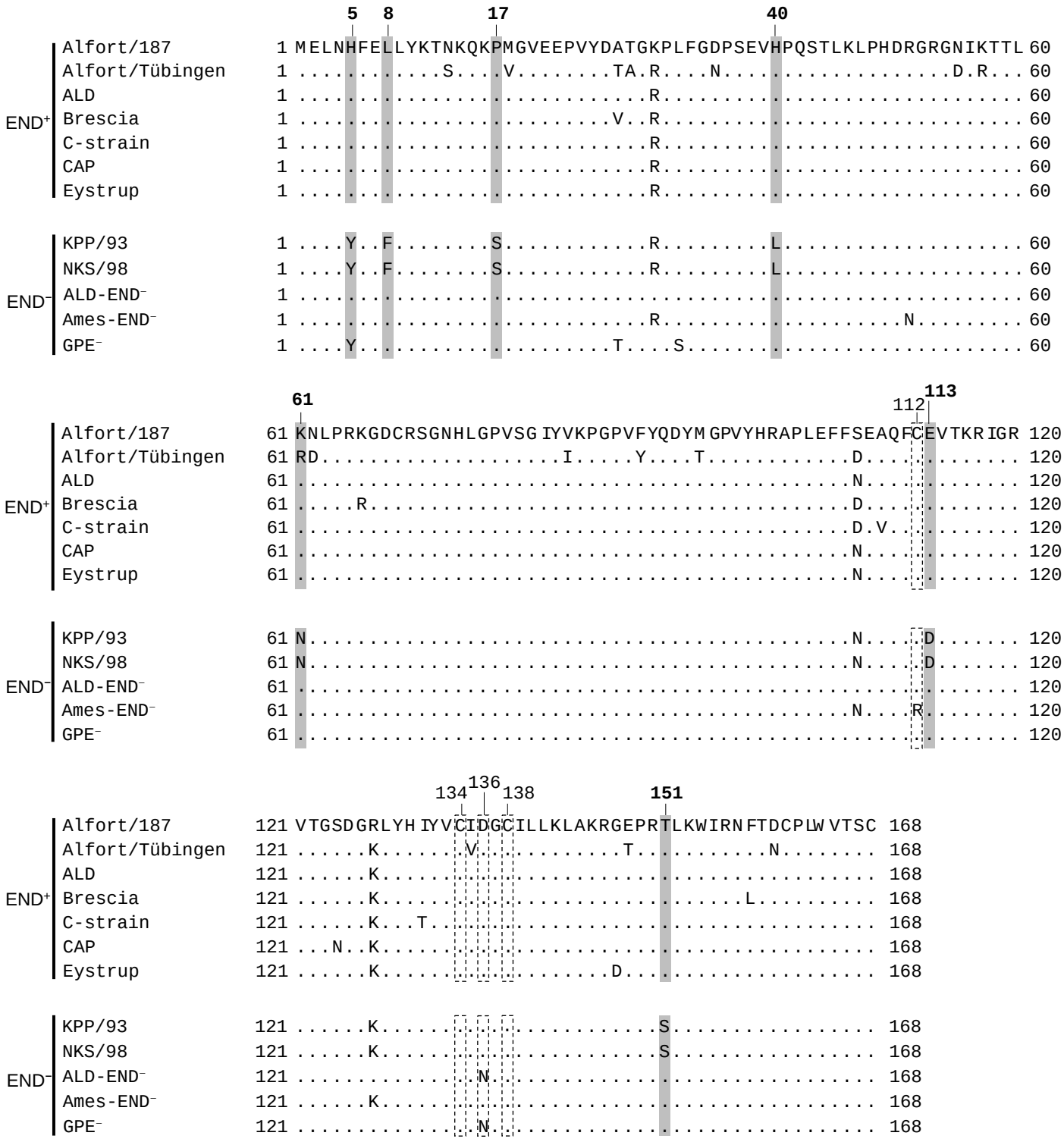

Figure 2, Mine *et al*.

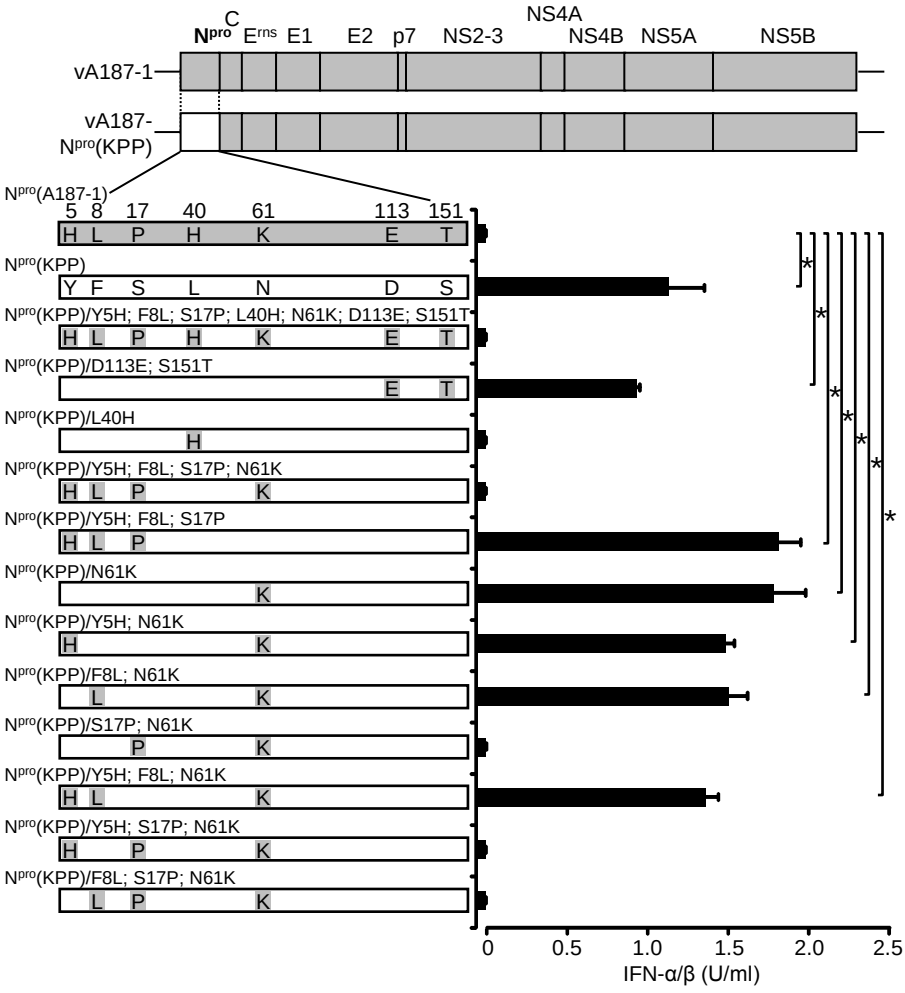

Figure 3, Mine *et al*.

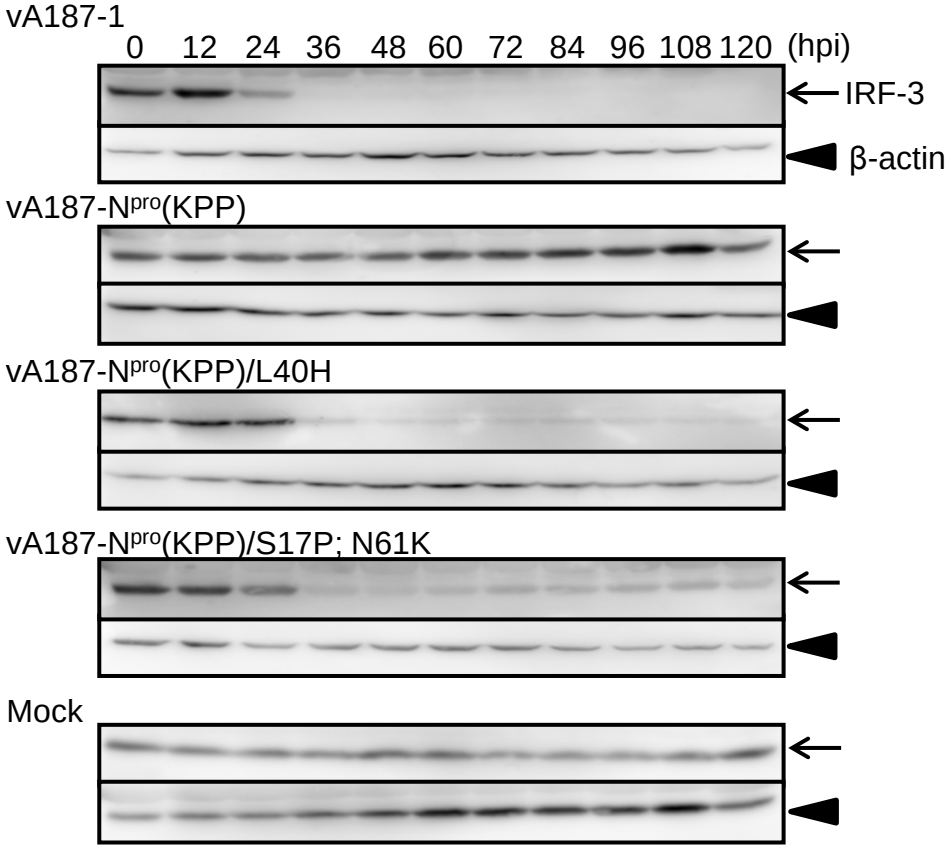

Figure 4, Mine *et al*.

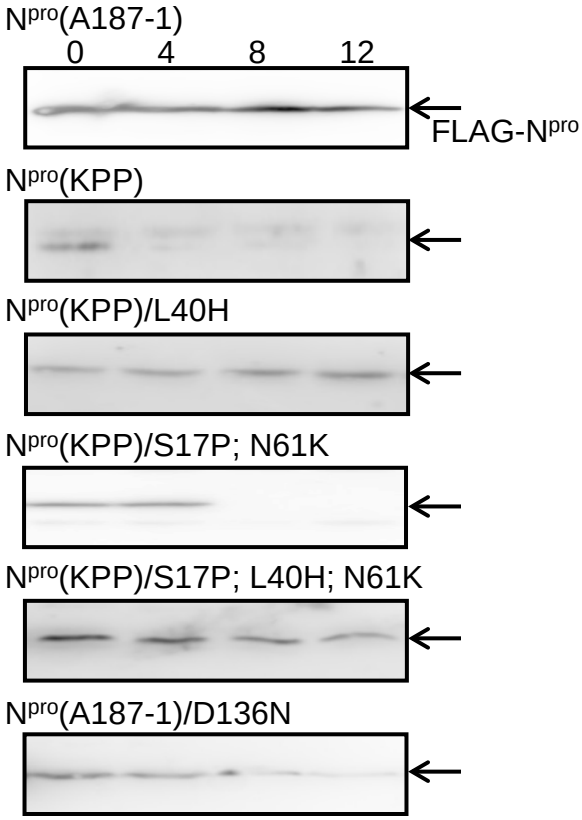

Figure 5, Mine *et al*.

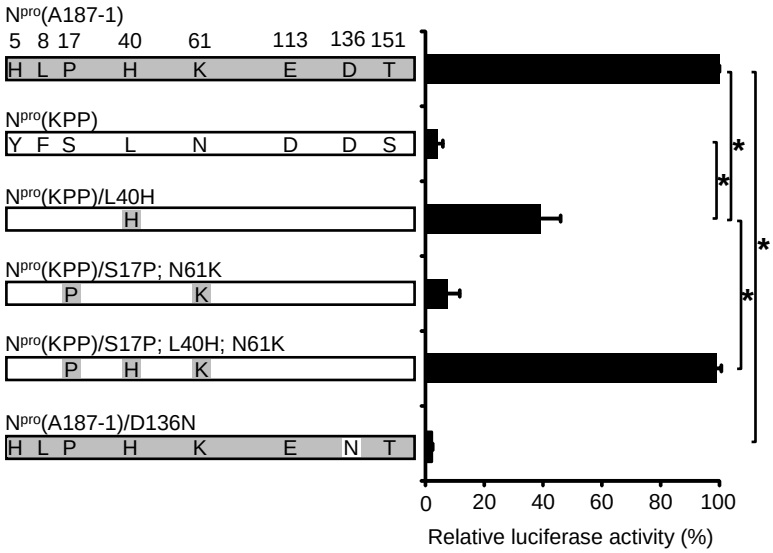

Figure 6, Mine *et al*.

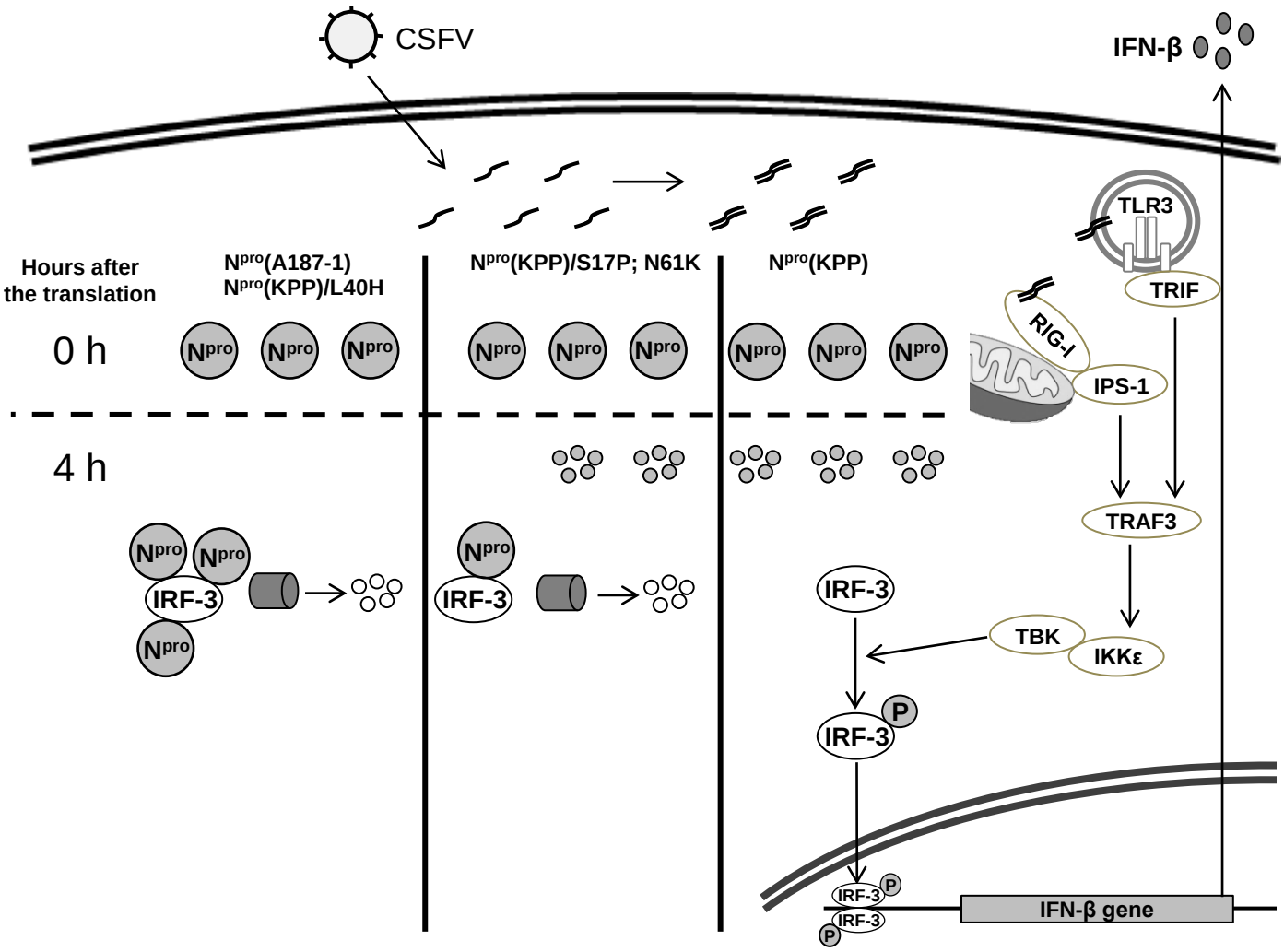

Figure 7, Mine *et al*.